Available online at www.sciencedirect.com
SCIENCE DIRECT®
Physics Letters B 626 (2005) 65–71
PHYSICS LETTERS B
www.elsevier.com/locate/physletb

Near-threshold measurement of the ^{4}He(γ, n) reaction

B. Nilsson [a], J.-O. Adler [a], B.-E. Andersson [a], J.R.M. Annand [b], I. Akkurt [b], M.J. Boland [a], G.I. Crawford [b], K.G. Fissum [a,1], K. Hansen [a], P.D. Harty [b], D.G. Ireland [b], L. Isaksson [a], M. Karlsson [a], M. Lundin [a], J.C. McGeorge [b], G.J. Miller [b], H. Ruijter [a], A. Sandell [a], B. Schröder [a], D.A. Sims [a], D. Watts [b]

[a] *Department of Physics, University of Lund, SE-221 00 Lund, Sweden*
[b] *Department of Physics and Astronomy, University of Glasgow, G12 8QQ Glasgow, UK*

Received 2 June 2005; received in revised form 12 August 2005; accepted 22 August 2005

Available online 29 August 2005

Editor: D.F. Geesaman

Abstract

A near-threshold ^{4}He(γ, n) cross-section measurement has been performed at MAX-lab. Tagged photons from $23 < E_\gamma < 42$ MeV were directed toward a liquid ^{4}He target, and neutrons were detected by time-of-flight in two liquid-scintillator arrays. Seven-point angular distributions were measured for eight photon energies. The results are compared to experimental data measured at comparable energies and Recoil-Corrected Continuum Shell Model, Resonating Group Method, and recent Hyperspherical-Harmonic Expansion calculations. The angle-integrated cross-section data are peaked at a photon energy of about 28 MeV, in disagreement with the value recommended by Calarco, Berman, and Donnelly in 1983.

PACS: 25.10.+s; 25.20.Lj

Keywords: ^{4}He(γ, n); Tagged photons; Time-of-flight; Cross section

Over the past several decades, many experiments have been performed in an attempt to understand the near-threshold photodisintegration of ^{4}He. In 1983, a review article by Calarco, Berman, and Donnelly (CBD) [1] assessed all available experimental data and made a recommendation as to the value of the ^{4}He(γ, n) cross section up to a photon energy of 50 MeV. Subsequently, the bulk of the experimental effort has been directed towards measuring either the ratio of the photoproton-to-photoneutron cross sections or simply the photoproton channel. In contrast, only two near-threshold measurements of the photoneutron channel have been published [2,3]. In this Letter, we report new results obtained for the

E-mail address: kevin.fissum@nuclear.lu.se (K.G. Fissum).
[1] Tel.: +46 46 222 8618; fax: +46 46 222 4709.

0370-2693
doi:10.1016/j.physletb.2005.08.081

^{4}He(γ, n) reaction near threshold, and compare them with the CBD evaluation as well as the post-CBD data. We also demonstrate consistency with previously published higher-energy tagged-photon data [4]. Finally, we compare our data to Recoil-Corrected Continuum Shell Model (RCCSM) calculations [5,6], a Resonating Group Method (RGM) calculation [7], and a recent Hyperspherical-Harmonic (HH) Expansion calculation [8]. A detailed description of the project summarized in this Letter is given in [9] and will be published in a full article [10].

The experiment was performed at the MAX-lab tagged-photon facility [11]. A 93 MeV, ∼30 nA, pulse-stretched electron beam with a duty factor of 75% was used to produce quasi-monoenergetic photons via the bremsstrahlung-tagging technique [12]. Post-bremsstrahlung electrons were momentum-analyzed in a magnetic spectrometer equipped with two 32-counter focal-plane scintillator arrays. These arrays tagged a photon-energy interval from $23 < E_\gamma < 42$ MeV with a FWHM energy resolution of ∼300 keV. The average instantaneous single-counter rate was 0.5 MHz, and the photon-beam collimation resulted in a tagging efficiency [11] of ∼25%.

A storage-cell cryostat held the liquid ^{4}He which constituted the target. The cylindrical 75 mm (high) ×90 mm (diameter) cell of 80 μm thick Kapton was mounted with the cylinder axis perpendicular to the photon-beam direction. The cell was surrounded by a heat shield of three layers of 30 μm thick Al foil and multiple layers of the super-insulation NRC-2, all maintained at liquid-N_2 temperature. The assembly sat in a vacuum chamber with 125 μm thick Kapton entrance and exit windows. An identical empty target cell on the movable target ladder enabled measurement of room and non-^{4}He background, which turned out to be negligible. Further, a 1 mm thick steel sheet, also mounted on the target ladder, was used to produce relativistic e^+e^- pairs for time-of-flight (TOF) calibration of the neutron detectors (see below). Density fluctuations in the liquid ^{4}He were negligible [13], as was the attenuation of the photon flux due to atomic processes within the target materials and the liquid ^{4}He [14].

Neutrons were detected in two large solid-angle spectrometers [15], each consisting of nine 20 cm × 20 cm × 10 cm deep rectangular cells mounted in a 3×3 lattice and filled with the liquid scintillator NE213A. Each of these arrays was mounted on a movable platform ($45 \text{ deg} < \theta_{\text{neutron}} < 135 \text{ deg}$) and encased in Pb, steel, and borated-wax shielding. Plastic scintillators which were 2 cm thick were placed in front of the liquid scintillators and used to identify incident charged particles. The average flight path to the NE213A arrays was 2.6 m, resulting in a 6 msr geometrical solid angle for a single cell and a FWHM TOF neutron-energy resolution of < 2 MeV, which allowed unambiguous identification of two-body ^{4}He(γ, n) events (see the overset in Fig. 1). Thus, the neutron energy also provided a cross check on the tagged-photon energy.

Gamma-ray sources were used to calibrate pulse-height output [15–17] from the NE213A scintillators which was necessary to determine the neutron-detection threshold and thus the neutron-detection efficiency. Pulse-shape discrimination (PSD) [18] was employed to distinguish neutrons from photons as the background photon flux on the TOF spectrometers was $\sim 10^5$ times greater than the neutron flux. All events not seen by the veto detector and identified as neutrons by the PSD modules generated a trigger for the data-acquisition system [19]. The data set for each neutron detector consisted of 64 TOF spectra containing real coincidences with the tagger focal plane and a random background (see the overset in Fig. 1). The ratio of prompt neutrons to random background (due mainly to photons which survived the PSD rejection and neutrons resulting from untagged bremsstrahlung) was a strong function of photon energy, ranging from 1-to-1 at $E_\gamma = 40.7$ MeV to 1-to-10 at $E_\gamma = 24.6$ MeV. The 64 TOF spectra were summed in eight groups of eight tagger counters resulting in ∼2.5 MeV wide photon-energy bins, each accumulating $\sim 10^{12}$ photons over the course of the measurement. The background was fitted by superimposing a periodic ripple (related to the electron beam circuit time within the pulse-stretcher ring [20]) upon an exponential distribution (due to dead-time effects in the detectors and the single-hit TDCs used to instrument the focal plane).

The background-subtracted neutron yield was corrected for tagger focal-plane dead-time effects [21]. A GEANT3-based Monte Carlo simulation [22] was used to determine the neutron-yield attenuation between the reaction vertex and the detector cells as well as the contribution of time-correlated background neutrons scattering into the detectors. The neutron-

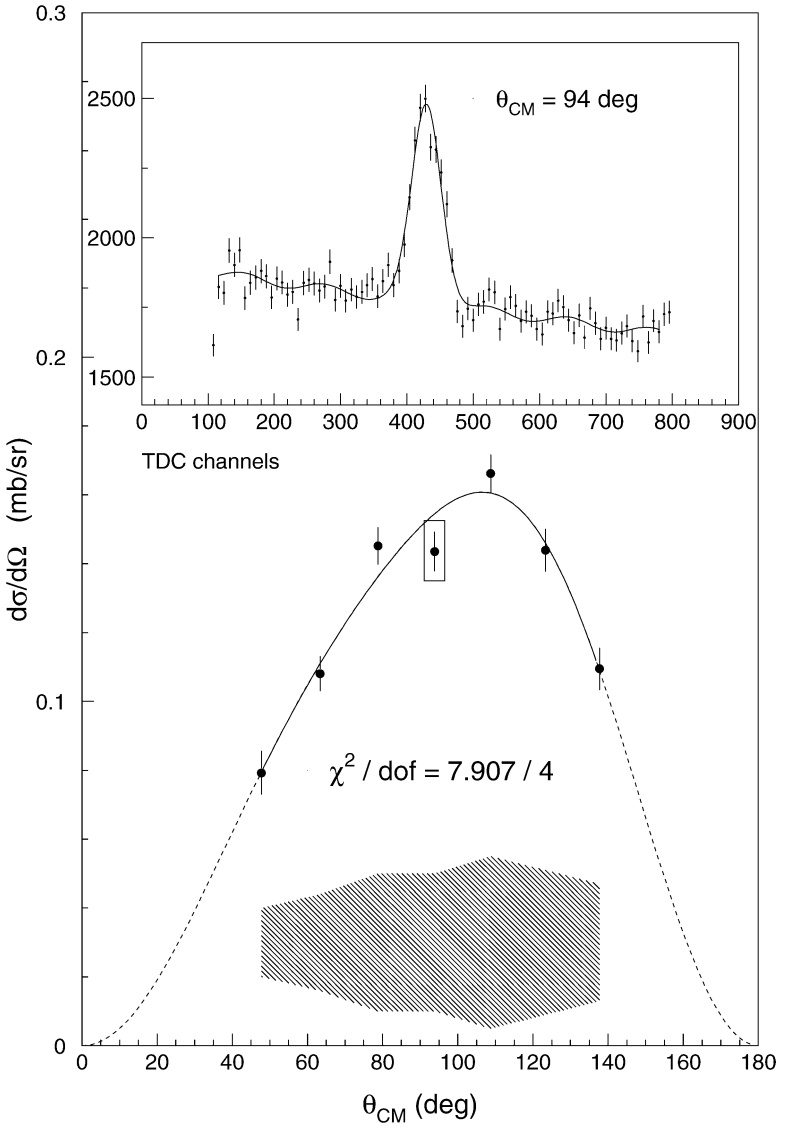

Fig. 1. An angular distribution measured at $E_\gamma = 28.8$ MeV. Error bars are the statistical uncertainties, while the systematic uncertainties are represented by the band at the base of the panel. Fitted function (Eq. (1)) — solid line; fitted function extrapolated to zero at $\theta_{\mathrm{CM}} = (0, 180)$ deg — dashed line. The TOF spectrum corresponding to the boxed data point at $\theta_{\mathrm{CM}} = 94$ deg is presented in the overset. The prominent peak corresponds to two-body neutron events. See text for details.

detection efficiency was determined using the STANTON Monte Carlo code [23]. Cross checks of the predictions made by GEANT3 and STANTON were performed via a dedicated measurement of the neutron-detection efficiency using a ^{252}Cf fission-fragment source [24]. A summary of the corrections applied to the cross-section data and the corresponding systematic uncertainties is presented in Table 1.

The angular distributions measured at each photon energy were converted from the laboratory to the center-of-mass (CM) frame and fitted using

$$\frac{d\sigma}{d\Omega}(\theta_{\mathrm{CM}}) = \alpha\left\{\sin^2(\theta_{\mathrm{CM}})\left[1+\beta\cos(\theta_{\mathrm{CM}})+\gamma\cos^2(\theta_{\mathrm{CM}})\right] + \delta + \epsilon\cos(\theta_{\mathrm{CM}})\right\} \quad (1)$$

Table 1
A summary of the correction factors applied to the cross-section data and the corresponding systematic uncertainties. In the case of the kinematic-dependent corrections, average values for the correction and the uncertainty are stated

kinematic-dependent quantity	⟨value⟩	⟨uncertainty⟩
neutron-detection efficiency	0.20	8%
neutron inscattering	1.25	9%
neutron-yield attenuation	0.85	6%
tagger focal-plane livetime	0.95	2%
neutron-detector livetime	0.50	1%
scale quantity	value	uncertainty
tagging efficiency	0.25	3%
particle misidentification	–	1%
photon-beam attenuation	–	1%

(see Fig. 1). This expansion assumes that the photon multipolarities are restricted to E1, E2, and M1, and that the nuclear matrix elements of the E-multipoles to final states with a channel spin of unity are negligible[2] [25]. Under these assumptions, α arises from the incoherent sum of the E1, E2, and M1 multipoles, β is due to the interference of the E1 and E2 multipoles, γ results from the E2 multipole, δ arises from the M1 multipole, and ϵ is zero. Similar to analyses of complementary ^{4}He(γ, p) angular distributions [25,27], our angular distributions were constrained to vanish at $\theta_{\mathrm{CM}} = (0, 180)$ deg by forcing the δ and ϵ coefficients to be zero.

Fig. 2 presents the α, β, and γ coefficients (filled circles) together with those extracted from a recent reanalysis [10] of the higher-energy data of Sims et al. [4] (open circles). We stress that these two data sets from MAX-lab are the only tagged-photon data in existence which are differential in angle. Error bars are the statistical uncertainties, while the systematic uncertainties are represented by the bands at the base of each panel. Also shown are RCCSM [5] and RGM [7] calculations. The recent HH calculation [8] does not presently predict angular distributions.

The RCCSM calculations were performed within a continuum shell-model framework in the $(1p1h)$ approximation, where the transition matrix elements of the M1 and the spin-independent M2 multipole operators vanished. Corrections were applied for target recoil. In addition to the Coulomb force, the effective nucleon–nucleon (NN) interaction included central, spin–orbit, and tensor components. Perturbation theory was employed to compute matrix elements for the multipoles and the multipole operators were calculated in the long-wavelength limit. Corrections for spurious CM excitations made these calculations essentially equivalent to the multichannel microscopic RGM calculations. Here, a similar semi-realistic NN force was employed, and the variational principle was used to determine the scattering wave functions. The radiative processes were treated within the Born Approximation, and the electromagnetic transition operators were again taken in the long-wavelength limit. Angular momenta up to $L = 2$ were allowed in the relative motion of the fragments. Note that the authors of the calculations originally presented their results in the form of Legendre coefficients as a function of CM proton energy.

As can be seen, the data largely reproduce the trends predicted by the calculations. At lower photon energies, the E1 multipole is completely dominant and the α data have a clear resonant structure peaking at about 28 MeV. The RCCSM calculation tends to overestimate these data, but also shows resonant structure peaking at about 25 MeV. The energy dependence of the β data is reasonably consistent with both the RCCSM and the RGM predictions, given the relatively large systematic uncertainties for $E_\gamma <$ 26 MeV. Similarly, when accuracy and precision are considered, there is no significant disagreement between the present γ data and the RCCSM calculation. At higher photon energies, E2 strength is expected to become more important. Unfortunately, the calculations do not cover the range of the higher-energy data. However, these data do appear to be consistent with the energy-dependent trends of both the lower-energy data and the calculations.

Fig. 3 presents the angle-integrated cross-section data (filled circles) together with those extracted from a recent reanalysis [10] of the higher-energy data of Sims et al. [4] (open circles). On average, these angle-integrated data are approximately 7% larger than those which result from simply scaling our $\theta_{\mathrm{CM}} = 90$ deg results by $8\pi/3$. Also shown is the CBD evaluation [1], data from a ^{3}He(n, γ) measurement [2], data from a ^{4}He$(\gamma, {}^3He)$ active-target measurement [3], a recent

[2] Note that Weller et al. [26] claim non-zero interfering E1 $S = 1$ strength.

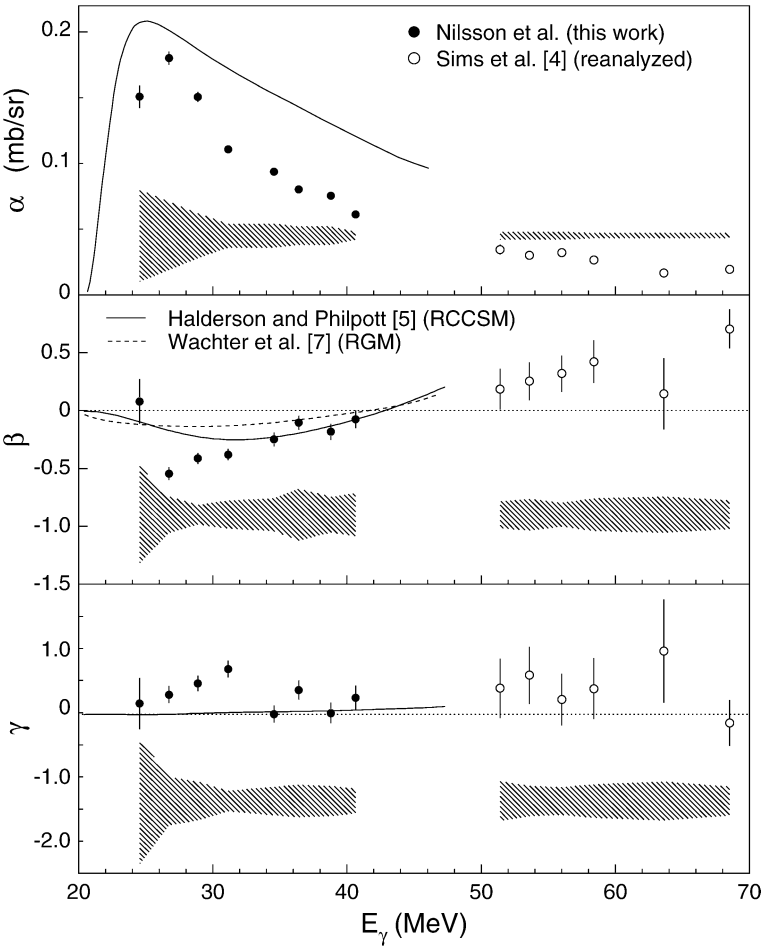

Fig. 2. The α, β, and γ coefficients: present data — filled circles; reanalyzed MAX-lab data [4,10] — open circles; RCCSM calculations [5] — solid lines; RGM calculation [7] — dashed line. See text for details.

RCCSM calculation [6], and the recent HH calculation [8]. Error bars show the statistical uncertainties, while the systematic uncertainties are represented by the bands at the base of the figure.

The recent RCCSM calculation expanded the model space of Ref. [5] to include more reaction channels and all p-shell nuclei. The HH calculation used a correlated hyperspherical expansion of basis states, with final-state interactions accounted for using the Lorentz Integral Transform Method (which circumvents the calculation of continuum states). For clarity, the small uncertainty in the HH calculation is not shown here. Note that both calculations employ the semirealistic MTI-III potential [28].

The present ^{4}He(γ, n) excitation function has a clear resonant structure peaking at about 28 MeV. Although data are lacking between 42 and 50 MeV, there is no apparent discontinuity with respect to the reanalyzed MAX-lab data of [4]. Furthermore, the present data extrapolate smoothly to the lower-energy data of [2]. Conversely, the data of [3] exhibit a slow rise which is at odds with all other data, the calculations, and the CBD evaluation. Both the RCCSM and HH calculations are in good agreement with the present data and those of [2] up to the resonant peak at $E_\gamma \sim$ 28 MeV. At higher energies, both calculations tend to overpredict the cross section, although the HH calculation follows the general shape of the excitation

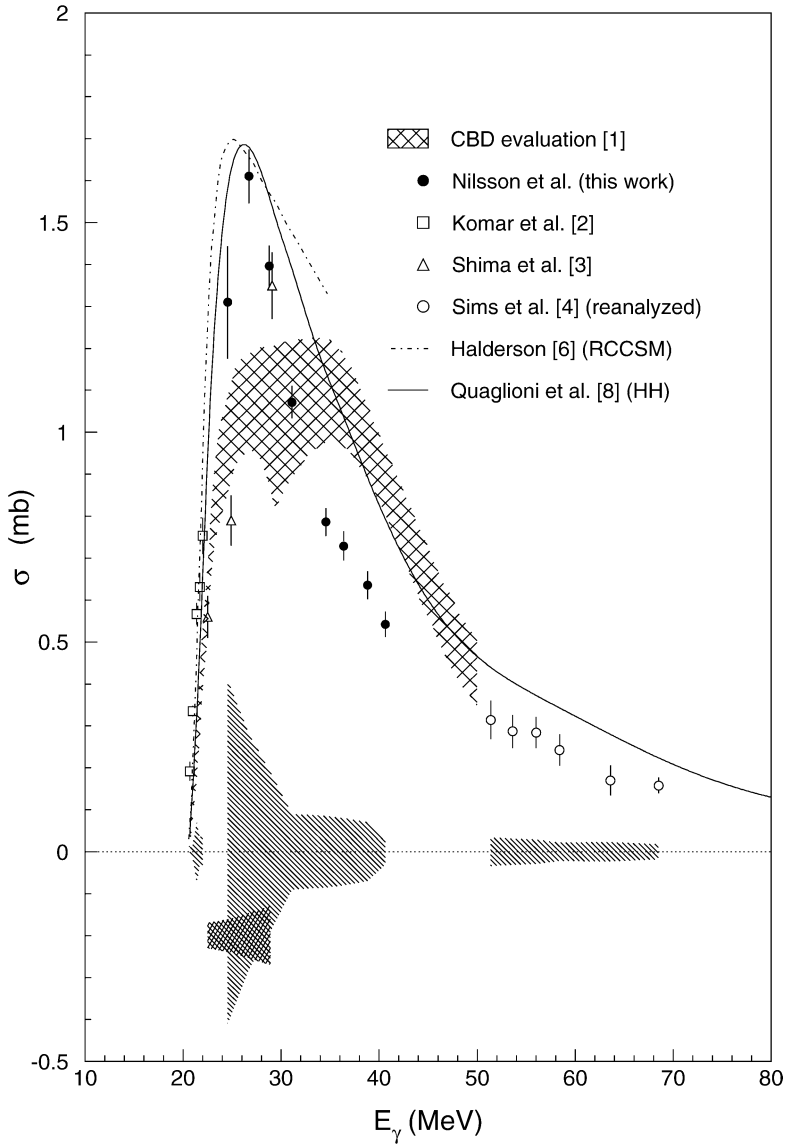

Fig. 3. The angle-integrated ^{4}He(γ, n) cross section: present data — filled circles; reanalyzed MAX-lab data [4,10] — open circles; CBD evaluation [1] — hatched band; recent RCCSM calculation [6] — dashed-dotted line; and HH calculation [8] — solid line. See text for details.

function up to 70 MeV reasonably well. Development of the HH formalism continues [29], and we anticipate new predictions in the near future which use fully realistic NN potential models and which may also include 3N-force effects.

In summary, $\frac{d\sigma}{d\Omega}(\theta)$ for the ^{4}He(γ, n) reaction have been measured with tagged photons and compared to other available measurements and calculations. The energy dependence of the α, β, and γ coefficients extracted from the angular distributions agrees reasonably with trends predicted by RCCSM [5] and RGM [7] calculations. The marked resonant behaviour of the present angle-integrated cross section, peaking at about 28 MeV, is in good agreement with recent RCCSM [6] and HH [8] calculations as well as capture data [2] which extend close to the (γ, n) threshold.

This behaviour disagrees with an evaluation of (γ, n) data [1] made in 1983, and recent active-target data [3].

Acknowledgements

The authors acknowledge the outstanding support of the MAX-lab staff which made this experiment successful. We also wish to thank Sofia Quaglioni, Winfried Leidemann, and Giuseppina Orlandini (University of Trento, Italy), John Calarco (University of New Hampshire, USA), Gerald Feldman (The George Washington University, USA), Dean Halderson (Western Michigan University, USA), Andreas Reiter (University of Glasgow, Scotland), and Brad Sawatzky (University of Virginia, USA) for valuable discussions. B.N. wishes to thank Margareta Söderholm and Ralph Hagberg for their unwavering support. The Lund group acknowledges the financial support of the Swedish Research Council, the Knut and Alice Wallenberg Foundation, the Crafoord Foundation, the Swedish Institute, the Wenner-Gren Foundation, and the Royal Swedish Academy of Sciences. The Glasgow group acknowledges the financial support of the UK Engineering and Physical Sciences Research Council.

References

[1] J.R. Calarco, B.L. Berman, T.W. Donnelly, Phys. Rev. C 27 (1983) 1866, and references therein.
[2] R.J. Komar, H.-B. Mak, J.R. Leslie, H.C. Evans, E. Bonvin, E.D. Earle, T.K. Alexander, Phys. Rev. C 48 (1993) 2375.
[3] T. Shima, Y. Nagai, T. Baba, T. Takahashi, T. Kii, H. Ohgaki, H. Toyokawa, Nucl. Phys. A 687 (2001) 127c.
[4] D.A. Sims, J.-O. Adler, J.R.M. Annand, G.I. Crawford, K.G. Fissum, K. Hansen, D.G. Ireland, L. Isaksson, S. McAllister, M. Lundin, J.C. McGeorge, B. Nilsson, H. Ruijter, A. Sandell, W. Sandhas, B. Schröder, S.A. Sofianos, Phys. Lett. B 442 (1998) 43.
[5] D. Halderson, R.J. Philpott, Nucl. Phys. A 359 (1981) 365, and references therein;
The calculation shown for α in the top panel of Fig. 2 was provided via private communication.
[6] D. Halderson, Phys. Rev. C 70 (2004) 034607, and references therein.
[7] B. Wachter, T. Mertelmeier, H.M. Hofmann, Phys. Rev. C 38 (1988) 1139, and references therein.
[8] S. Quaglioni, W. Leidemann, G. Orlandini, N. Barnea, V.D. Efros, Phys. Rev. C 69 (2004) 044002, and references therein.
[9] B. Nilsson, PhD thesis, University of Lund, Sweden, 2003, unpublished;
See also http://www.maxlab.lu.se/kfoto/publications/nilsson.pdf.
[10] B. Nilsson, et al., Phys. Rev. C, submitted for publication.
[11] J.-O. Adler, B.-E. Andersson, K.I. Blomqvist, K.G. Fissum, K. Hansen, L. Isaksson, B. Nilsson, D. Nilsson, H. Ruijter, A. Sandell, B. Schröder, D.A. Sims, Nucl. Instrum. Methods A 388 (1997) 17.
[12] J.-O. Adler, B.-E. Andersson, K.I. Blomqvist, B. Forkman, K. Hansen, L. Isaksson, K. Lindgren, D. Nilsson, A. Sandell, B. Schröder, K. Ziakas, Nucl. Instrum. Methods A 294 (1990) 15.
[13] M.W. Tate, M.E. Sadler, Nucl. Instrum. Methods 204 (1983) 295.
[14] E. Storm, H.I. Israel, Nucl. Data Tables A 7 (1970) 565.
[15] J.R.M. Annand, B.-E. Andersson, I. Akkurt, B. Nilsson, Nucl. Instrum. Methods A 400 (1997) 344.
[16] K.F. Flynn, L.E. Glendenin, E.P. Steinberg, P.M. Wright, Nucl. Instrum. Methods 27 (1964) 13.
[17] H.H. Knox, T.G. Miller, Nucl. Instrum. Methods 101 (1972) 519.
[18] J.R.M. Annand, Nucl. Instrum. Methods A 262 (1987) 371.
[19] H. Ruijter, PhD thesis, University of Lund, Sweden, 1995, unpublished;
See also http://www.maxlab.lu.se/kfoto/publications/ruijter.pdf.
[20] L. Van Hoorebeke, D. Ryckbosch, C. Van den Abeele, R. Van de Vyver, J. Dias, Nucl. Instrum. Methods A 326 (1993) 608.
[21] D. Hornidge, PhD thesis, University of Saskatchewan, Canada, 1999, unpublished;
See also www.mta.ca/~dhornidg/phd_thesis.pdf.
[22] http://wwwasd.web.cern.ch/wwwasd/geant.
[23] N.R. Stanton, A Monte Carlo Program for calculating neutron detection efficiencies in plastic scintillator, Ohio State University Preprint COO-1545-92, Columbus, OH, USA, 1971.
[24] M. Karlsson, Diploma thesis, University of Lund, Sweden, 1997, unpublished;
See also http://www.maxlab.lu.se/kfoto/publications/karlsson_xjobb.pdf.
[25] R.T. Jones, D.A. Jenkins, P.T. Debevec, P.D. Harty, J.E. Knott, Phys. Rev. C 43 (1991) 2052, and references therein.
[26] H.R. Weller, N.R. Robertson, G. Mitev, L. Ward, D.R. Tilley, Phys. Rev. C 25 (1982) 2111.
[27] J. Calarco, private communication.
[28] R.A. Malfliet, J. Tjon, Nucl. Phys. A 127 (1969) 161.
[29] G. Orlandini, private communication.